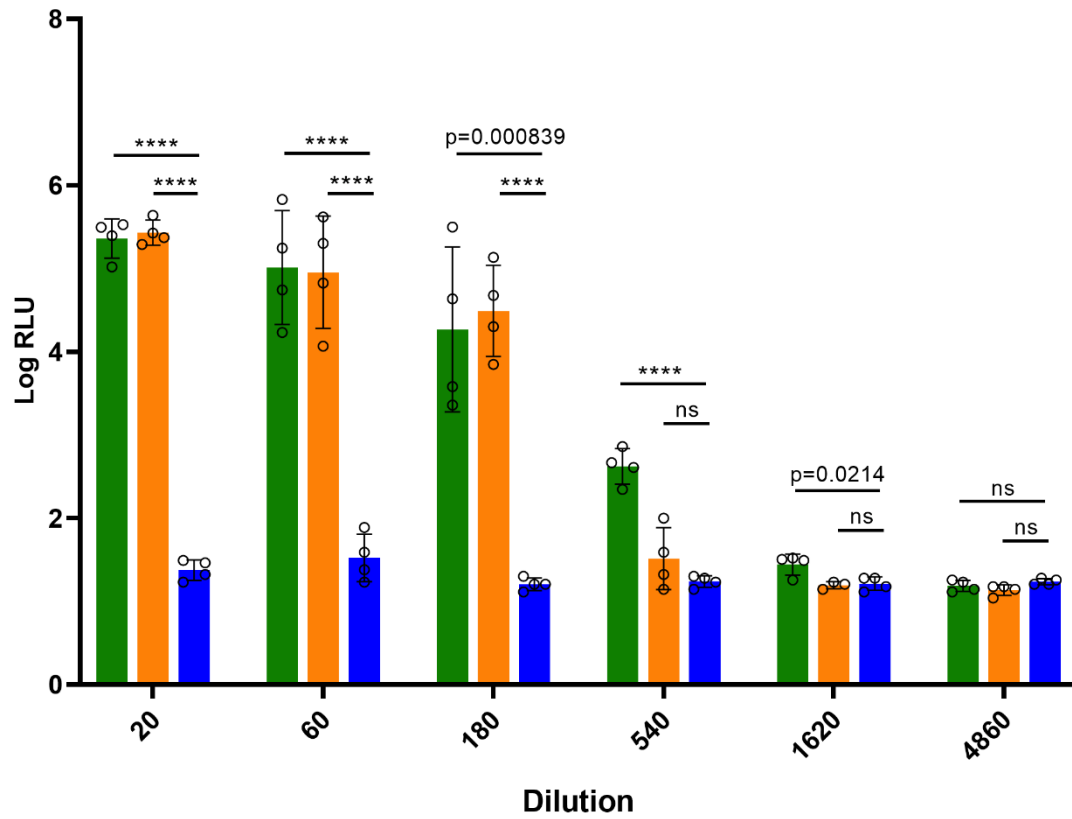


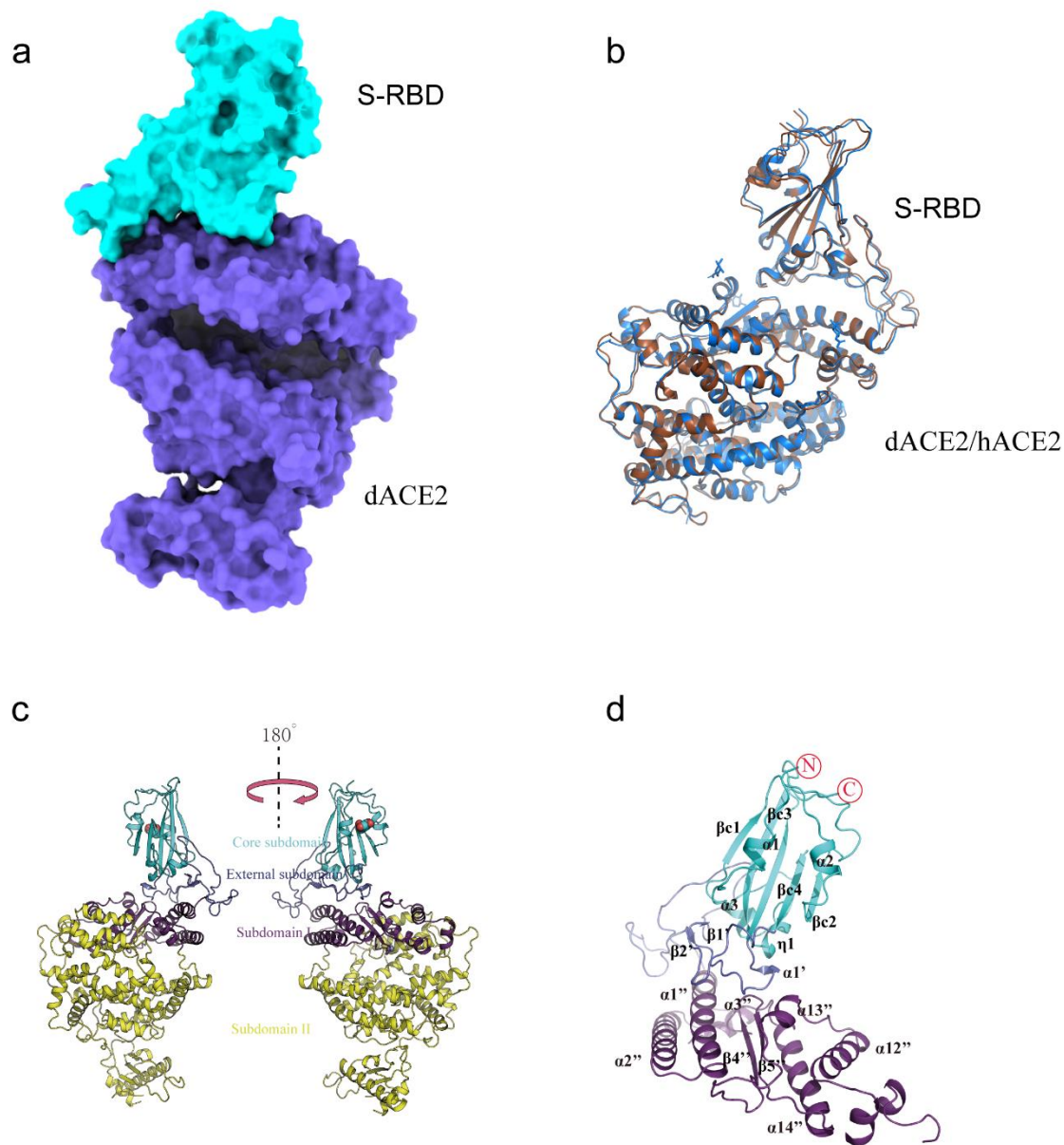
Supplementary Information

Supplementary Figure 1



Supplementary Figure 1. Infection of dACE2- or hACE2-expressing HeLa cells with the SARS-CoV-2 S protein-bearing pseudovirus. Data are presented as mean values \pm SD of quadruplicate cell samples. ****, $p < 0.0001$; ns means no significant differences; two-sided Student's *t*-test.

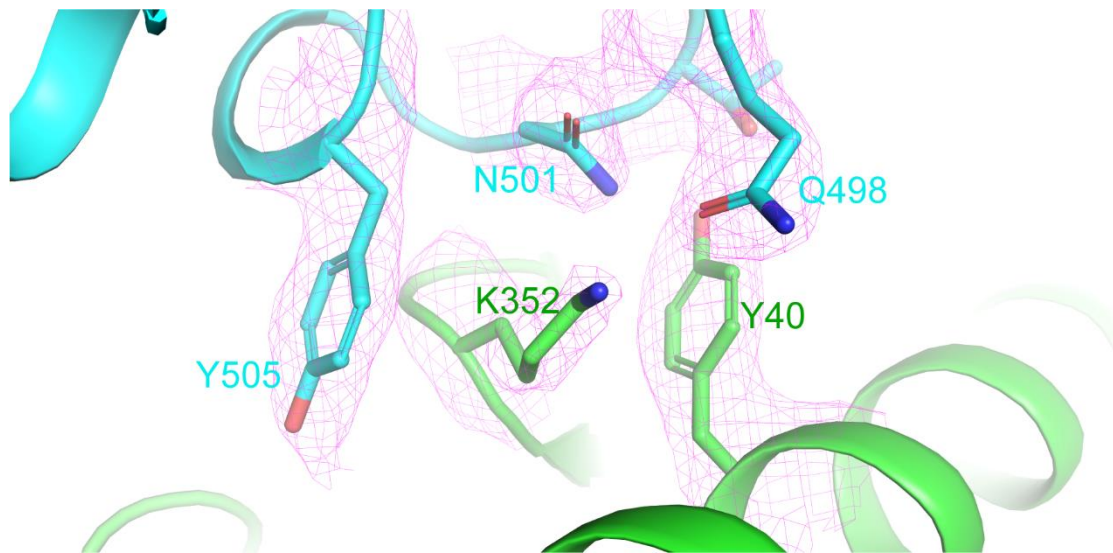
Supplementary Figure 2



Supplementary Figure 2. The crystal structure of the RBD/dACE2 complex. (a) The overall crystal structure of the RBD/dACE2 complex. RBD is labeled in cyan and dACE2 in blue. (b) Alignment of the RBD/dACE2 complex (brown) to the RBD/hACE2 complex (marine, PDB ID: 6LZG). (c) The subdomains of RBD and dACE2 at two side viewpoints of 180° rotation. The RBD core subdomain, RBD external subdomain, dACE2 subdomain I and dACE2 subdomain II are colored with cyan, slate, purple, and yellow, respectively. (d) The secondary structural elements in

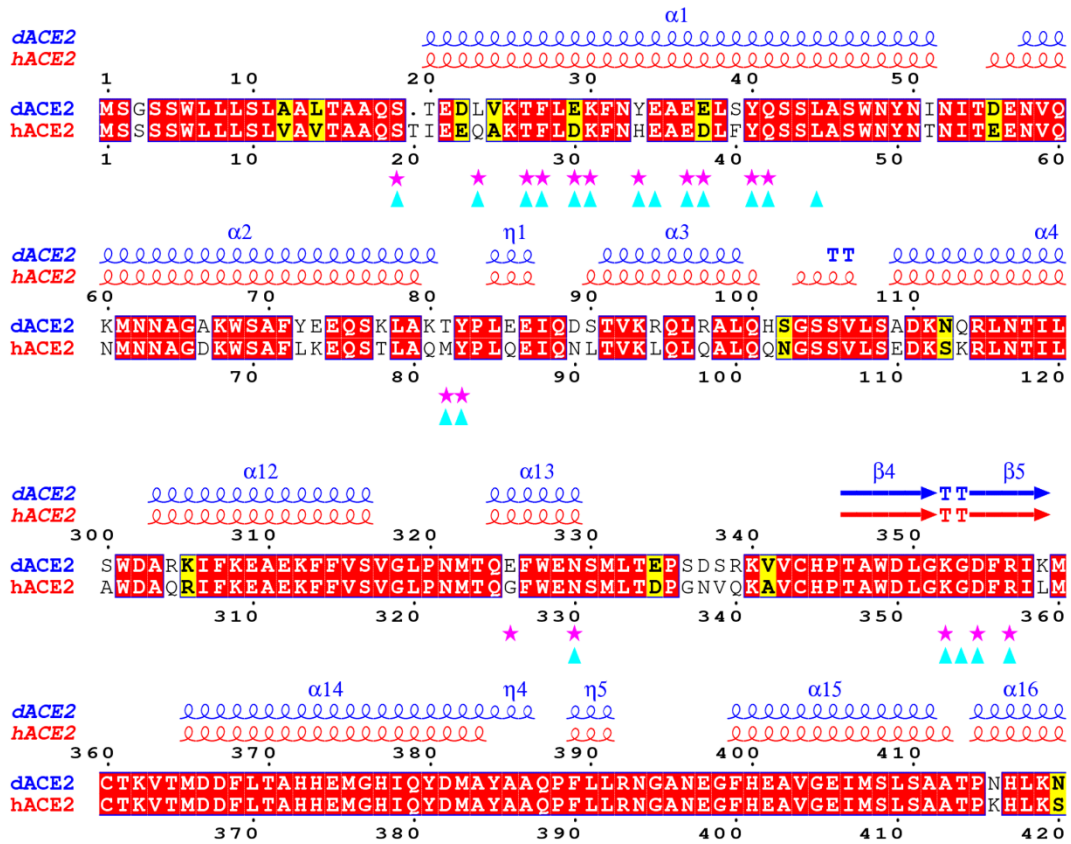
the RBD and dACE2 subdomain I in the complex. The subdomains are colored the same as in (c).

Supplementary Figure 3



Supplementary Figure 3. The local 2Fo-Fc electronic density map at 1.0 σ for the binding interface in the RBD/ dACE2 complex. The electronic density is represented as pink mesh. RBD is shown as cyan and dACE2 is shown as green.

Supplementary Figure 4



Supplementary Figure 4. Sequence alignment of dACE2 and hACE2. The dACE2 residues that contact with RBD in the RBD/ dACE2 are shown as hot pink stars. The hACE2 residues that make contact with RBD in the RBD/ hACE2 are shown as cyan triangles. The sequence alignment was performed with MEGAX¹ and visualized with ESPrpt². The columns with residues in white and the background in red indicate a strict identity, and the columns with residues in black and the background in yellow indicate a similarity score over 0.7, considering the physio-chemical property.

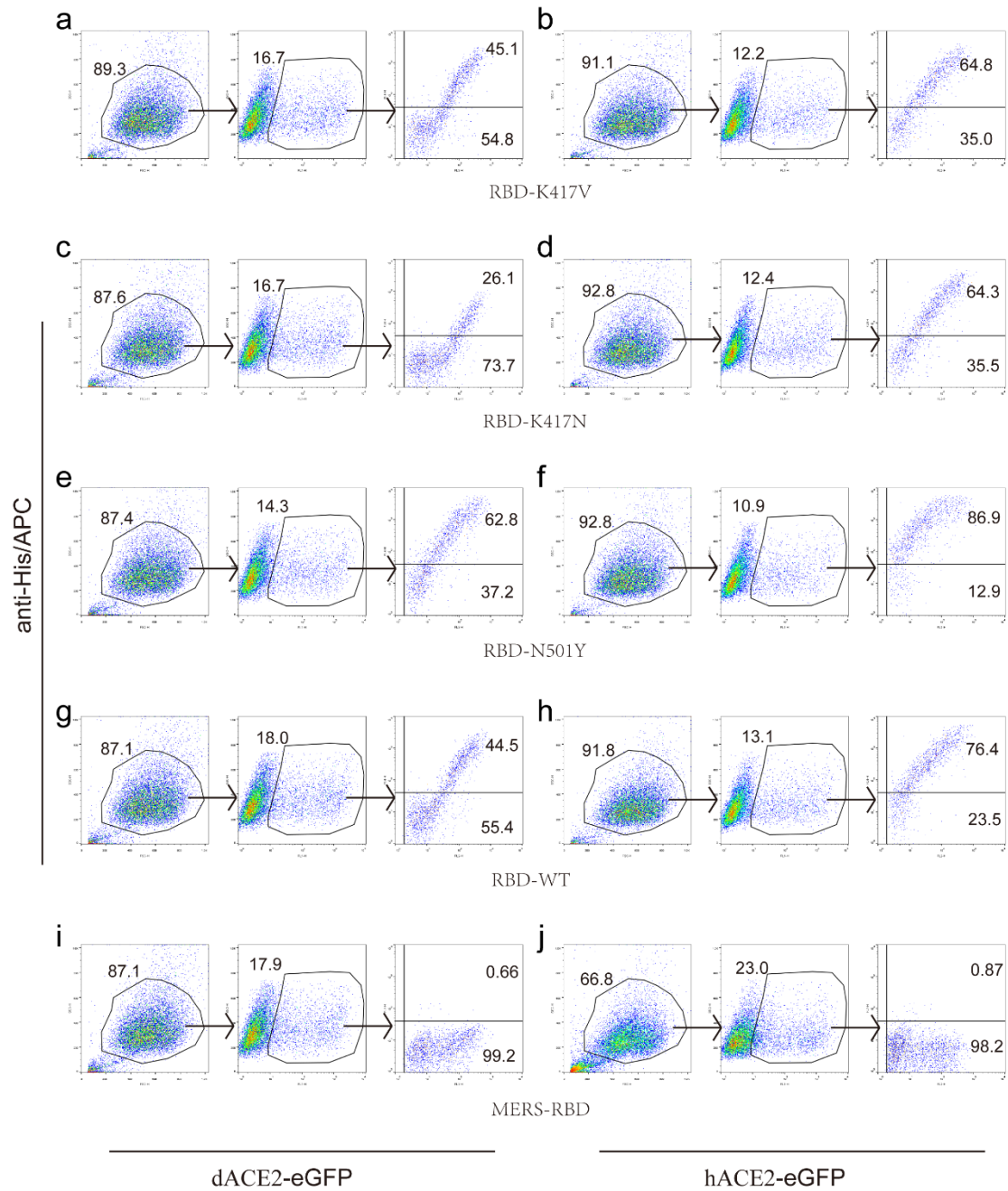
Supplementary Figure 5

		417
a	hCoV-19/Wuhan/WIV04/2019	I A P G Q T G K I A D
	hCoV-19/Germany/BY-MGZ-03/2020	I A P G Q T G N I A D
	hCoV-19/England/QEUIH-9983ED/2020	I A P G Q T G N I A D
	hCoV-19/Scotland/QEUIH-96CEC3/2020	I A P G Q T G N I A D
	hCoV-19/pangolin/Guangxi/P1E/2017	I A P G Q T G V I A D
	hCoV-19/pangolin/Guangxi/P4L/2017	I A P G Q T G V I A D
b		501
	hCoV-19/Wuhan/WIV04/2019	Y G F Q P T N G V G Y
	hCoV-19/USA/MA-JLL-D152/2020	Y G F Q P T Y G V G Y
	hCoV-19/England/CAMC-B533FB/2020	Y G F Q P T Y G V G Y
	hCoV-19/Wales/PHWC-4897BB/2020	Y G F Q P T Y G V G Y
	hCoV-19/Wales/PHWC-47DA93/2020	Y G F Q P T Y G V G Y
	hCoV-19/Australia/VIC2173/2020	Y G F Q P T Y G V G Y

Supplementary Figure 5. Alignment of parts of the RBD amino acid sequences from different strains containing the relevant mutations tested in the present study.

(a) Alignment of SARS-CoV-2 S protein containing the K417N and the K417V mutations with the reference sequence (hCoV-19/Wuhan/WIV04/2019). (b) Alignment of SARS-CoV-2 S protein contain the N501Y mutation with the reference sequence (hCoV-19/Wuhan/WIV04/2019). The sequence alignment was prepared with MEGAX¹. The residue positions 417 (a) and 501 (b) are highlighted in different colors.

Supplementary Figure 6



Supplementary Figure 6. The gating strategy for flow cytometry analysis of SARS-CoV-2 RBD interface residue mutants, wt RBD, or MERS-CoV RBD binding to BHK21 cells expressing dACE2 or hACE2. The cells expressing dACE2-eGFP (a, c, e, g, i) or hACE2-eGFP (b, d, f, h, j) were incubated with His-tagged RBD K417V mutant (a and b), RBD K417N mutant (c and d), RBD N501Y (e and f), wt RBD (g and h) or MERS-CoV RBD (i and j), respectively. The cells were the strained with the anti-

His/APC antibody and subjected to flow cytometry analysis. The cells populated based on the forward scatter (FSC) and the side scatter (SSC) signals were first gated with the eGFP fluorescent densities. The eGFP⁺ cell population were further divided into the APC⁺ population (cells binding to RBD or its mutants) and APC⁻ population (cells not binding to RBD or its mutants). The percentages of the APC⁺ eGFP⁺ cells and the APC⁻ eGFP⁺ cells in the eGFP⁺ cells are indicated.

Supplementary Table 1. Data collection and refinement statistics

SARS2-CoV-2 RBD/dACE2	
Data collection	
Space group	I422
Cell dimensions	
<i>a, b, c</i> (Å)	168.26, 168.26, 211.20
α, β, γ (°)	90.00, 90.00, 90.00
Resolution (Å)	50.00-3.00 (3.11-3.00)
Unique reflections	30355 (2989)
Completeness (%)	98.5 (99.5)
R_{merge}	0.18.4 (0.599)
$I/\sigma I$	8.8 (2.6)
CC _{1/2} (%)	0.980 (0.819)
Redundancy	6.3 (6.2)
Refinement	
Resolution (Å)	48.26-3.00
No. reflections	29668
$R_{\text{work}} / R_{\text{free}}$	0.2272/0.2479
No. atoms	
Protein	7244
Ligand/ion	1
Water	0
<i>B</i> -factors	
Protein	52.6
Ligand/ion	76.8
Water	
R.M.S. deviations	
Bond lengths (Å)	0.002
Bond angles (°)	0.531
Ramchandran	
Statistics (%)	
Favored	96.49
Allowed	3.51
Disallowed	0.00

Values in parentheses are for the highest resolution shell.

Supplementary Table 2. Comparison of residue contacts of SARS-CoV-2 RBD binding to dACE2 and hACE2

SARS-CoV-2 RBD	dACE2	hACE2
R403 (1/0)	Y33(1)	-
K417 (2, <u>1</u> /3, <u>1</u>)	E29 (1, <u>1</u>)	D30 (3, <u>2</u>)
G446 (1, <u>1</u> /1, <u>1</u>)	Q41 (0, <u>1</u>)	Q42 (1)
Y449 (6, <u>2</u> /8, <u>2</u>)	E37 (4, <u>1</u>), Q41 (0, <u>1</u>)	D38 (5, <u>1</u>), Q42 (1, <u>1</u>)
Y453 (6/3)	Y33 (6)	H34 (3)
L455 (3/4)	E29(1), Y33 (2)	H34 (4)
F456 (4/7)	T26 (3), E29 (1)	T27 (5), D30 (1), K31 (1)
A475 (3/5, <u>1</u>)	L23(2), T26(1)	S19 (3,1), Q24 (1), T27 (1)
G476 (0/2)		S19 (2)
F486 (10/11)	T81(3), T82 (7)	M82 (4), Y83 (7)
N487 (4, <u>1</u> /11, <u>2</u>)	L23 (1), Y82 (3, <u>1</u>)	Q24 (7, <u>1</u>), Y83 (4, <u>1</u>)
Y489 (7/7, <u>1</u>)	T26 (1), F27 (3), K30 (2), Y82 (1)	T27 (2), F28 (4), Y83 (0, <u>1</u>)
F490 (0/ <u>1</u>)		K31 (0, <u>1</u>)
Q493 (0/8, <u>1</u>)		H34 (3), E35 (4, <u>1</u>)
G496 (6, <u>1</u> /2, <u>1</u>)	E37 (2), K352 (4, <u>1</u>)	D38 (1), K353 (1, <u>1</u>)
Q498 (10, <u>2</u> /19, <u>1</u>)	E37 (2, <u>1</u>), Y40(3), Q41 (2, <u>1</u>), K352(3, <u>1</u>)	D38(1), Y41(7), Q42(9, <u>1</u>), L45(2)
T500 (17, <u>2</u> /17, <u>1</u>)	Y40 (6, <u>1</u>), N329(4), D354 (6, <u>1</u>), R356 (1)	Y41 (5, <u>1</u>), N330 (3), D355 (5), R357 (3)
N501 (11, <u>1</u> /10, <u>2</u>)	Y40 (5, <u>1</u>), E325(1), K352(5)	Y41 (5, <u>1</u>), K353 (4, <u>1</u>)
G502 (7, <u>1</u> /8, <u>1</u>)	K352 (2, <u>1</u>), G353(5)	K353 (3, <u>1</u>), G354 (5)
Y505 (27, <u>2</u> /20, <u>1</u>)	E36(7, <u>1</u>), K352 (18), R392(1, <u>1</u>)	E37 (2, <u>1</u>), K353 (15), G354 (2), R392(1)
Q506(1, <u>1</u> /0)	E325(1, <u>1</u>)	
Total	127, <u>13</u>	145, <u>16</u>

The numbers in parentheses of SARS-CoV-2 RBD residues represent the number of vdw and H-bond/salt bridges contacts between the indicated residue with dACE2 (the former) and hACE2 (the latter). The numbers in parentheses of ACE2 residues represent the numbers of vdw contacts the indicated residues conferred. The numbers with underlines suggest numbers of potential H-bonds or salt bridges between the pairs of residues. Vdw contacts were analyzed at a cutoff of 4 Å. H-bonds/salt bridges were analysis with PDBePISA (<https://www.ebi.ac.uk/pdbe/pisa/>)

Supplementary Table 3. Hydrogen bonds and salt bridges at the binding interfaces of in the dACE2/SARS-CoV-2 RBD and the hACE2/ SARS-CoV-2 RBD complexes (*)

	dACE2/SARS-CoV-2 RBD complex						hACE2/ SARS-CoV-2 RBD complex					
	Chain B			Distance	Chain A		No.	Residue	Atom	Distance	Residue	Atom
No.	Residue	Atom	Residue		Atom	Residue						
Hydrogen bond	1	K417	NZ	3.25	E29	OE1	1	K417	NZ	2.86	D30	OD1
	2	Y449	OH	2.66	E37	OE2	2	Y449	OH	3.09	Q42	OE1
	3	N487	ND2	3.16	Y82	OH	3	Y449	OH	2.83	D38	OD1
	4	Q498	NE2	2.92	E37	OE2	4	N487	ND2	2.82	Y83	OH
	5	T500	OG1	2.43	Y40	OH	5	Y489	OH	3.54	Y83	OH
	6	N501	N	3.73	Y40	OH	6	Q493	NE2	3.39	E35	OE1
	7	G502	N	2.92	K352	O	7	Q498	NE2	2.57	Q42	OE1
	8	Y505	OH	2.52	E36	OE2	8	T500	OG1	2.73	Y41	OH
	9	Q506	NE2	3.59	E325	OE2	9	N501	N	3.62	Y41	OH
	10	G446	O	3.61	Q41	NE2	10	G502	N	2.79	K353	O
	11	Y449	OH	3.36	Q41	NE2	11	Y505	OH	3.66	E37	OE1
	12	G496	O	2.97	K352	NZ	12	A475	O	2.81	S19	OG
	13	Y505	OH	3.6	R392	NH2	13	N487	OD1	2.87	Q24	NE2
							14	F490	O	3.82	K31	NZ
							15	G496	O	3.22	K353	NZ
Salt bridge	1	K417	NZ	3.25	E29	OE1	1	K417	NZ	3.76	D30	OD2
							2	K417	NZ	2.86	D30	OD1

(*) H-bonds/salt bridges were analysis with PDBEPIISA (<https://www.ebi.ac.uk/pdbe/pisa/>)

Supplementary Table 4. Codon optimized gene sequence for proteins expression

1. dACE2, tagged with 6xHis, cloned into pET21a with NdeI and XhoI

CATATGCAGTCAACAGAAGATCTTGTTAAGACGTTTCCTTGAGAAGTTCAATTATGAAGCTGAAGAAGCTTTCATAT
CAGTCATCACTTGCTTCATGGAACATAACATTAACATTACAGATGAGAATGTCCAGAAGATGAATAACGCTGGC
GCTAAATGGTCAGCTTCTACGAGGAACAGTCAAAGCTAGCAAAGACTTACCCTCTTGAAGAAATTCAGGATTC
AACAGTTAAACGCCAGCTTCGCGCTCTTCAGCATTACAGGCTCATCAGTTCTTTCAGCTGATAAGAATCAACGCCT
TAACACAATTCTTAACCTCAATGTCAACAATTATTCAACAGGCAAAGCTTGTAAACCCTTCAAACCCTCAGGAATG
TCTTCTTCTGAACTGGTCTGGACGACATAATGGAGAATAGTAAGGACTACAACGAACGCCTTTGGGCTTGGGA
AGGCTGGCGCTCAGAAGTTGGCAAACAGCTTCGCCCTCTTATGAAGAATATGTTGCTCTTAAGAATGAGATGGC
TCGCGCTAAACAATATGAAGATTATGGCGATTATTGGCGCGCGATTATGAAGAAGAATGGGAGAATGGATATAA
CTATTCACGCAACCAGCTTATTGATGATGTTGAACATACATTTACACAGATTATGCCTCTTATCAGCATCTTCATG
CTTATGTTTCGCAAAAAGCTAATGGATACATATCCTTCATATATTTACCTACAGGCTGTCTTCCCTGCTCATCTTCTG
GCGATATGTGGGGACGGTTCTGGACCAACCTTTATCCTCTTACAGTTCCTTTTCGGTCAGAAGCCAAATATTGATGT
TACAAACGCTATGGTTAACCAGTCATGGGATGCTCGCAAGATCTTTAAGGAGGCTGAGAAGTTCTTCGTTTCGGT
TGGCCTTCTAACATGACACAGGAATTCTGGGAGAACTCAATGCTTACAGAACCTTCAGATTCACGCAAAGTTGT
TTGTCATCTACAGCTTGGGATCTTGGCAAAGGCGATTTCGGATCAAGATGTGCACAAAGGTGACGATGGATGA
TTTCTGACCGCTCATCATGAAATGGGCCATATTCAGTATGATATGGCTTATGCTGCTCAGCCTTCTCTTACGCA
ACGGCGCTAACGAAGGCTTTCATGAAGCTGTTGGCGAAATTATGTCACCTTTCAGCTGCTACACCTAACCATCTTA
AGAATATAGGCCTTCTTCTCCTTCATCTTTCGAGGACTCAGAAACAGAAATTAACCTTCTTCTTAAACAGGCTCT
TACAATTGTTGGCACACTTCTTTCACGTACATGCTTGAGAAGTGGCGTTGGATGGTATTCAAGGGTGAGATCCC
TAAAGATCAGTGGATGAAGACTTGGTGGGAAATGAAACGCAACATTGTTGGCGTTGTTGAACCTGTTCCCTCATG
ATGAAACATATTGTGATCCTGCTTCACTGTTCCACGTGGCTAACGATTATTCATTTATTCGCTATTATACACGCACA
ATTTATCAGTTTCAGTTTCAGGAAGCTCTTGTGATGCTAAACATGAAGGCCCTTTCATAAATGTGATATTT
AAACTCATCAGAAGCTGGCCAGAACTTCTTGAATGCTTAAACTTGGCAAATCAAAGCCGTGGACTTATGCTC
TTGAAATTGTTGTTGGCGCTAAGAATATGGATGTTTCGCCCTCTTCTTAACTATTTTCGAGCCGCTTCTCACTTGGCTT
AAAGAACAGAACCACAACCTCATTGTTGGCTGGAACACAGATTGGTCACCTTATGCTGATCAGTCAATTAAGTT
CGCATTTCACTTAAATCAGCTCTTGGCGAGAAGGCCTACGAATGGAACAACAACGAAATGTATCTCTCAGATCT
TCAATTGCTTATGCTATGCGCCAGTATTTCTCCGAGGTTAAGAATCAAACAATTCCTTTCGTCGAGGATAACGTTT
GGGTTTCAGATCTTAAACCTCGCATTTTCACTTAACTTCTTCGTCACCTCACCTGGCAACGTTTCAGATATTATTCCT
CGCACAGAAGTTGAAGAAGCTATTCGCATGTATCGCTCACGCATTAACGATGTATTCCGGCTAGACGACAATAGT
CTTGAATTTCTTGGCATTACGCTACACTTGGCCCTCTTATGAACCTCCTGTTACACATCATCATCATCATCATCATG
ACTCGAG

2. hACE2, fused with mFc, cloned into pCAGGS with NdeI and XhoI

CATATGTCAACAATTGAAGAACAGGCTAAGACCTTCCTTGATAAATTTAACCATGAAGCTGAAGATCTCTTCTACC
AATCATCACTTGCTTCATGGAACATAACACAAACATTACAGAAGAGAATGTCCAGAACATGAACAACGCTGGC
GATAAATGGTCAGCTTTCTTGAAGGAACAGTCAACACTTGCTCAGATGTATCCTCTTCAGGAAATTCAGAACCTT
ACAGTTAACTTCAGCTTCAGGCTCTCAGCAGAATGGTTCTTCGGTGTATCAGAAGATAAATCAAAGAGGCTC
AACACAATTCTTAACACAATGTCAACAATTTATTCAACAGGCAAAGTTTGTAACCCTGATAACCCTCAGGAATGT
CTTCTTCTTGAACCTGGCCTTAACGAAATTATGGCTAACTACTTGATTATAACGAACGCCTTTGGGCTTGGGAAT
CATGGCGCTCAGAAGTTGGCAAACAGCTTCGCCACTCTATGAGGAGTACGTTGTTCTTAAGAATGAGATGGCTC
GCGCTAACCAATTATGAAGATTATGGCGATTATTGGCGCGGCGATTATGAAGTTAACGGCGTTGATGGCTATGATTAT
TCACGCGCCAGCTTATTGAAGATGTTGAACATACATTTGAAGAAATTAACCGCTCTACGAGCACTTGCATGCT
TATGTTGCGCTAAACTTATGAACGCTTATCCTTCATATATTTACCTATTGGCTGTCTTCTGCTCATCTTCTTGGC
GATATGTGGGGTCGTTTTTGGACGAACCTTTATTCACCTACAGTTCCTTTCCGACAGAAGCCGAATATTGATGTTA
CAGATGCTATGGTTGATCAGGCTTGGGATGCTCAGCGCATATTCAAGGAGGCTGAGAAGTTCTTCGTTTCGGTGTG
GCCTTCTAACATGACACAGGGCTTCTGGGAGAACTCAATGCTTACAGATCCTGGCAACGTTTCAGAAAGCTGTT
TGTCATCCTACAGCTTGGGATCTTGGCAAAGGCGATTTACAGATCCTTATGTGTACAAAGGTAACCTATGGATGATT
TCCTAACCGCACACCAGAGATGGGCCATATTCAGTATGATATGGCTTATGCTGCTCAGCCTTTCCTGTTACGCCAA
CGGCGCTAACGAAGGCTTTCATGAAGCTGTTGGCGAAATATGTCACCTTCAGCTGCTACACCTAAACATCTTAA
ATCAATTGGCCTTCTTTCACCTGATTTCCAAGAGGATAACGAAACAGAAATTAACCTTCTTCTTAAACAGGCTCTT
ACAATTGTTGGCACACTTCCTTTCACCTACATGCTTGAGAAGTGGCGGTGGATGGTATTCAAGGGTGAAATTCCT
AAAGATCAGTGGATGAAGAAGTGGTGGGAAATGAAACGCGAAATGTTGGCGTGTGTTGAACCTGTTCTCTCATGA
TGAAACATATTGTGATCCTGCTTCATTGTTCCACGTATCAAACGATTATTCATTTATTCGCTATTATACACGCACACT
TTATCAGTTTCAGTTTCAGGAAGCTCTTGTGTCAGGCTGCTAAACATGAAGGCCCTTTCATAAATGTGATATTCA
AACTCAACAGAAGCTGGCCAGAACTGTTCAATATGCTTCGCCTTGGCAAATCAGAACCTTGGACACTTGCTCT
TGAGAATGTAGTTGGCGCTAAGAATATGAACGTTCCGCCTTCTTAACTATTTCCGAGCCGTTATTACGTGGCTT
AAAGATCAGAACAAGAATAGTTTCGTAGGGTGGTCAACAGATTGGTACCTTATGCTGATCATCATCATCATCATC
ATTGACTCGAG

3. SARS-CoV-2 RBD wt, tagged with 6xHis, cloned into pCAGGS with EcoRI and XhoI

ATGTTTGTGTTTCTTGTGCTTCTTCTCTTGTGTCATCACAATGCAGAGTGCAACCTACAGAATCAATCGTGAGAT
TTCCTAACATCACAAACCTTTGCCCTTTCGGCGAGGTGTTAACGCAACAAGATTGTCATCAGTGTACGCATGGA
ACAGAAAGCGTATATCAAACCTGCGTGGCAGATTACTCAGTGCTTTACAACCTCAGCATCATTAGTACGTTTAAAT
GCTACGGAGTGTACCTACAAAGCTAAATGATCTTTGCTTTACAAACGTGTACGCAGATTCATTTGTGATCAGAG
GAGATGAAGTGAGACAAATCGCACCTGGACAAACAGGAAAGATTGCCGATTACAACCTACAAACTTCTCTGATGAT
TTCACCGGCTGCGTGATCGCATGGAACCTAAACAACCTTGATTCAAAGGTAGGTGGTAATTATAATTATTTGTATA
GGCTCTTTCGTAAGAGCAACTTAAAGCCATTTGAGCGAGATATCTCAACAGAAATCTACCAAGCAGGATCAACA
CCTTGCAACGGAGTGAAGGATTTAACTGCTACTTTCCTCTTCAATCATACGGATTTCAACCTACAAACGGAGTG
GGATACCAACCTTACAGAGTGGTGGTCTTTCATTTGAACTTCTTACGCACCTGCAACAGTGTGCGGACCTAAG
AAGAGCACGAACCTTGTGAAGAATAAGTGCCTGAACTTTCACCACCACCACCCTGA

4. SARS-CoV-2 RBD wt, tagged with 6xHis, cloned into pFASTBACTM1 with EcoRI and XhoI

ATGTTTGTGTTTCTTGTGCTTCTTCCTCTTGTGTCATCACAATGCAGAGTGCAACCTACAGAATCAATCGTGAGAT
TTCCTAACATCACAAACCTTTGCCCTTTTCGGCGAGGTGTTAACGCAACAAGATTTGCATCAGTGTACGCATGGA
ACAGAAAGCGTATATCAAACCTGCGTGGCAGATTACTCAGTGCTTTACAACCTCAGCATCATTAGTACGTTTAAAT
GCTACGGAGTGTACCTACAAAGCTAAATGATCTTTGCTTTACAAACGTGTACGCAGATTCATTTGTGATCAGAG
GAGATGAAGTGAGACAAATCGCACCTGGACAAACAGGAAAGATTGCCGATTACAACCTACAACCTCCTGATGAT
TTCACCGGCTGCGTGTATCGCATGGAACCTCAAACAACCTTGATTCAAAGGTAGGTGGTAATTATAATTATTGTATA
GGCTCTTTTCGTAAGAGCAACTTAAAGCCATTTGAGCGAGATATCTCAACAGAAATCTACCAAGCAGGATCAACA
CCTTGAACGGAGTGGAAGGATTTAACTGCTACTTTCCTCTTCAATCATAACGGATTTCACCTACAACGGAGTG
GGATACCAACCTTACAGAGTGGTGGTCTTTCATTTGAACTTCTTACGCACCTGCAACAGTGTGCGGACCTAAG
AAGAGCACGAACCTTGTGAAGAATAAGTGCGTGAACCTTTCACCACCACCACCACCTGA

5. SARS-CoV-2 RBD K417V, tagged with 6xHis, cloned into pCAGGS with EcoRI and XhoI

GAATTCGCCACCATGTTTGTGTTTCTTGTGCTTCTTCCTCTTGTGTCATCACAATGCAGAGTGCAACCTACAGAAT
CAATCGTGAGATTTCTAACATCACAAACCTTTGCCCTTTTCGGCGAGGTGTTAACGCAACAAGATTTGCATCAG
TGTACGCATGGAACAGAAAGCGTATATCAAACCTGCGTGGCAGATTACTCAGTGCTTTACAACCTCAGCATCATTCA
GTACGTTTAAATGCTACGGAGTGTACCTACAAAGCTAAATGATCTTTGCTTTACAAACGTGTACGCAGATTCATT
TGTGATCAGAGGAGATGAAGTGAGACAAATCGCACCTGGACAAACAGGAGTGATTGCCGATTACAACCTACAAA
CTTCTGATGATTTACCGGCTGCGTGATCGCATGGAACCTCAAACAACCTTGATTCAAAGGTAGGTGGTAATTATA
ATTATTTGTATAGGCTCTTTCGTAAGAGCAACTTAAAGCCATTTGAGCGAGATATCTCAACAGAAATCTACCAAGC
AGGATCAACACCTTGCAACGGAGTGGAAGGATTTAACTGCTACTTTCCTCTTCAATCATAACGGATTTCACCTAC
AAACGGAGTGGGATACCAACCTTACAGAGTGGTGGTCTTTCATTTGAACTTCTTACGCACCTGCAACAGTGT
GCGGACCTAAGAAGAGCACGAACCTTGTGAAGAATAAGTGCGTGAACCTTTCACCACCACCACCACCTGACT
CGAG

6. SARS-CoV-2 RBD K417N, tagged with 6xHis, cloned into pCAGGS with EcoRI and XhoI

GAATTCGCCACCATGTTTGTGTTTCTTGTGCTTCTTCCTCTTGTGTCATCACAATGCAGAGTGCAACCTACAGAAT
CAATCGTGAGATTTCTAACATCACAAACCTTTGCCCTTTTCGGCGAGGTGTTAACGCAACAAGATTTGCATCAG
TGTACGCATGGAACAGAAAGCGTATATCAAACCTGCGTGGCAGATTACTCAGTGCTTTACAACCTCAGCATCATTCA
GTACGTTTAAATGCTACGGAGTGTACCTACAAAGCTAAATGATCTTTGCTTTACAAACGTGTACGCAGATTCATT
TGTGATCAGAGGAGATGAAGTGAGACAAATCGCACCTGGACAAACAGGAAACATTGCCGATTACAACCTACAAA
CTTCTGATGATTTACCGGCTGCGTGATCGCATGGAACCTCAAACAACCTTGATTCAAAGGTAGGTGGTAATTATA
ATTATTTGTATAGGCTCTTTCGTAAGAGCAACTTAAAGCCATTTGAGCGAGATATCTCAACAGAAATCTACCAAGC
AGGATCAACACCTTGCAACGGAGTGGAAGGATTTAACTGCTACTTTCCTCTTCAATCATAACGGATTTCACCTAC
AAACGGAGTGGGATACCAACCTTACAGAGTGGTGGTCTTTCATTTGAACTTCTTACGCACCTGCAACAGTGT
GCGGACCTAAGAAGAGCACGAACCTTGTGAAGAATAAGTGCGTGAACCTTTCACCACCACCACCACCTGACT
CGAG

7. SARS-CoV-2 RBD 501Y, tagged with 6xHis, cloned into pCAGGS with EcoRI and XhoI

GAATTCGCCACCATGTTTGTGTTTCTTGTGCTTCTTCTCTTGTGTCATCACAATGCAGAGTGCAACCTACAGAAT
CAATCGTGAGATTTCTAACATCACAAACCTTTGCCCTTTCGGCGAGGTGTTAACGCAACAAGATTTGCATCAG
TGTACGCATGGAACAGAAAGCGTATATCAAACCTGCGTGGCAGATTACTCAGTGCTTTACAACCTCAGCATCATTCA
GTACGTTTAAATGCTACGGAGTGTACCTACAAAGCTAAATGATCTTTGCTTTACAAACGTGTACGCAGATTCAAT
TGTGATCAGAGGAGATGAAGTGAGACAAATCGCACCTGGACAAACAGGAAAGATTGCCGATTACAACCTACAAA
CTTCTGATGATTTACCCGGCTGCGTGATCGCATGGAACCTCAAACAACCTTGATTCAAAGGTAGGTGGTAATTATA
ATTATTTGTATAGGCTCTTTCGTAAAGAGCAACTTAAAGCCATTTGAGCGAGATATCTCAACAGAAATCTACCAAGC
AGGATCAACACCTTGCAACGGAGTGGAAGGATTTAACTGCTACTTTCCTCTTCAATCATAACGGATTTCAACCTAC
ATACGGAGTGGGATACCAACCTTACAGAGTGGTGGTGCTTTCATTGAACTTCTTACGCACCTGCAACAGTGTG
CGGACCTAAGAAGAGCACGAACCTTGTGAAGAATAAGTGCCTGAACTTTCACCACCACCACCACCCTGACTC
GAG

8. MERS-CoV RBD, tagged with 6xHis, cloned into pCAGGS with EcoRI and XhoI

GAATTCGCAAAACCTTCTGGCTCAGTTGTGGAACAGGCTGAAGGTGTTGAATGTGATTTTTCACCTCTTCTGTCT
GGCACACCTCCTCAGGTTTATAATTTCAAGCGTTTGGTTTTTACCAATTGCAATTATAATCTTACCAAATTGCTTTC
ACTTTTTTCTGTGAATGATTTTACTTGTAGTCAAATATCTCCAGCAGCAATTGCTAGCAACTGTTATTCTTCACTGA
TTTTGGATTACTTTTTCATACCCACTTAGTATGAAATCCGATCTCAGTGTTAGTTCTGCTGGTCCAATATCCCAGTTT
AATTATAACAGTCCTTTTCTAATCCCACATGTTTGATTTTAGCGACTGTTCTCATAACCTTACTACTATTACTAAG
CCTCTTAAGTACAGCTATATTAACAAGTGCTCTCGTCTTCTTCTGATGATCGTACTGAAGTACCTCAGTTAGTGA
ACGCTAATCAATACTCACCTGTGTATCCATTGTCCCATCCACTGTGTGGGAAGACGGTGATTATTATAGGAAACA
ACTATCTCCACTTGAAGGTGGTGGCTGGCTTGTGTAGTGGCTCAACTGTTGCCATGACTGAGCAATTACAGAT
GGGCTTTGGTATTACAGTTCAATATGGTACAGACACCAATAGTGTGTTGCCCAAGCTTGAATTTGCTAATGACACA
AAAATTGCCTCTCAATTAGGCAATTGCGTGGAATATTCCCACCACCACCACCACCCTGACTCGAG

Supplementary References

1. Kumar S, Stecher G, Li M, Knyaz C, Tamura K. MEGA X: molecular evolutionary genetics analysis across computing platforms. *Mol Biol Evol* **35**, 1547-1549. (2018).
2. Robert X, Gouet P. Deciphering key features in protein structures with the new ENDscript server. *Nucleic Acids Res* **42**, W320-324. (2014).